HHS Public Access

Author manuscript

J Control Release. Author manuscript; available in PMC 2019 May 10.

Published in final edited form as:

J Control Release. 2018 May 10; 277: 14–22. doi:10.1016/j.jconrel.2018.03.001.

Ocular drug delivery targeted by iontophoresis in the suprachoroidal space using a microneedle

Jae Hwan Jung[1], **Bryce Chiang**[2,3], **Hans E. Grossniklaus**[4], and **Mark R. Prausnitz**[1,2,*]

[1]School of Chemical and Biomolecular Engineering, Georgia Institute of Technology, Atlanta, GA 30332, USA

[2]Wallace H. Coulter Department of Biomedical Engineering at Georgia Tech and Emory University, Georgia Institute of Technology, Atlanta, GA 30332, USA

[3]Emory University School of Medicine, Atlanta, GA 30329, USA

[4]Department of Ophthalmology, Emory University School of Medicine, Atlanta, GA 30322, USA

Abstract

Treatment of many posterior-segment ocular indications would benefit from improved targeting of drug delivery to the back of the eye. Here, we propose the use of iontophoresis to direct delivery of negatively charged nanoparticles through the suprachoroidal space (SCS) toward the posterior pole of the eye. Injection of nanoparticles into the SCS of the rabbit eye ex vivo without iontophoresis led to a nanoparticle distribution mostly localized at the site of injection near the limbus and <15% of nanoparticles delivered to the most posterior region of SCS (>9 mm from the limbus). Iontophoresis using a novel microneedle-based device increased posterior targeting with >30% of nanoparticles in the most posterior region of SCS. Posterior targeting increased with increasing iontophoresis current and increasing application time up to 3 min, but further increasing to 5 min was not better, probably due to the observed collapse of the SCS within 5 min after injection ex vivo. Reversing the direction of iontophoretic flow inhibited posterior targeting, with just ~5% of nanoparticles reaching the most posterior region of SCS. In the rabbit eye in vivo, iontophoresis at 0.14 mA for 3 min after injection of a 100 uL suspension of nanoparticles resulted in ~30% of nanoparticles delivered to the most posterior region of the SCS, which was consistent with ex vivo findings. The procedure was well tolerated, with only mild, transient tissue effects at the site of injection. We conclude that iontophoresis in the SCS using a microneedle has promise as a method to target ocular drug delivery within the eye, especially toward the posterior pole.

Graphical abstract

*To whom correspondence should be sent: prausnitz@gatech.edu.

Supporting Information

Supporting Information is available from the Wiley Online Library or from the author.

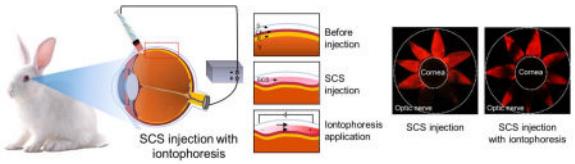

Iontophoresis in the suprachoroidal space using a microneedle has promise as a method to target ocular drug delivery to the back of the eye.

Keywords

Iontophoresis; Microneedle; Ocular drug delivery; Posterior segment; Suprachoroidal injection; Targeted drug delivery

1. Introduction

Ocular drug delivery to the back of the eye have been widely investigated to treat eye diseases such as macular edema, diabetic retinopathy and age-related macular degeneration [1–4]. Although various therapeutics have been developed and shown to be effective, they are generally not targeted to their sites of action, e.g., the macula [5–7], which may limit their safety and efficacy. Systemic oral or parenteral administration delivers drug throughout the body with high risk of side effects. Ocular drug delivery by topical eye drops, subconjunctival injection, and intravitreal injection, more effectively target the eye, but do not specifically target the macula or other target sites within the eye. Intravitreal injection has become increasingly popular for drug delivery to the posterior segment [1, 8]. However, this method not only exposes the whole posterior segment to drug without targeting specific sites of action typically around the posterior pole, but also delivers drug to more anterior tissues, such as the ciliary body, lens and cornea. Thus, new ocular drug delivery methods are needed to target the choroid/retina within the macula and/or near the optic disc is essential, which can increase drug efficacy and reduce side effects.

Injection into the suprachoroidal space (SCS) has been studied as a means to better target drug delivery specifically to the choroid and retina [1, 9, 10]. The SCS is a potential space between the choroid and sclera. Injection into this space allows drug to flow circumferentially at the choroid-sclera interface typically from an anterior injection site near the limbus and flowing posteriorly towards the posterior pole. While delivery can be targeted to the SCS using hypodermic needles, catheters and other devices often requiring surgical procedures performed under monitored anesthesia [11–15], the most progress in the field has been made by SCS injection using a hollow microneedle [16–19].

Microneedles for SCS delivery have been designed with a length similar to scleral thickness (e.g., < 1 mm), so that perpendicular insertion into the sclera positions the needle tip at the sclera-choroid junction with direct access the SCS in a minimally invasive way [7, 17, 18, 20]. From the SCS, drugs can access sites of action such as macula and optic disc at high concentration and without obstructing the visual axis, which can be caused by injecting material intravitreally, thereby targeting delivery to reduce side effects and enhance

bioavailability [11, 12, 21–25]. SCS injection with a microneedle has been studied in human subjects with excellent safety and tolerability in several clinical trials. Specifically, triamcinolone acetonide has been injected as a monotherapy into the SCS in patients with macular edema associated with non-infectious uveitis [26] currently in a Phase III clinical trial [27] and has been administered in combination with intravitreal injection of an anti-VEGF drug (aflibercept) in patients with retinal vein occlusion, currently in a Phase III clinical trial [28] and in patients with diabetic macular edema, currently in a phase I/II clinical trials [29]. While drug delivery via the SCS has promise, more work is needed to fully understand its strengths and weaknesses.

While SCS injection targets drug delivery to choroid and retina, it does not specifically target the posterior pole, e.g., macula [17–19, 30, 31]. Moreover, typical SCS injection volumes (e.g., ≤ 100 μL in the rabbit eye) are insufficient to flow injected drugs around the macula or optic disk [32–34]. Thus, greater targeting efficiency within the SCS could provide still better safety and efficacy, which is a current limitation of SCS injection.

To advance drug targeting to posterior SCS, a previous study introduced a gravity-mediated drug delivery method where high-density particle-stabilized emulsion droplets were designed to deliver drugs to the back of the eye via the SCS using gravity [19]. Drug formulations with hyaluronic acid were also developed, which spread throughout up to 100% of the SCS by a slow process after injection [30]. To target the anterior portion of the SCS, another study increased viscosity of the drug formulation using carboxymethyl cellulose to localize drugs near the ciliary body to treat glaucoma [34].

Another method of drug delivery to the eye involves iontophoresis, which can be used for posterior segment delivery [35–44]. In this noninvasive method, electric current is applied at the conjunctiva to transfer charged molecules into ocular tissues mediated by repulsive and attractive forces between charged molecules and electrodes [45–47]. However, due to the ocular tissue barriers, iontophoresis is not well suited to deliver macromolecules and particles into the eye, which limits application of this technique more broadly [1, 23, 48–50].

Guided by prior work with SCS injection and iontophoresis, we hypothesize that iontophoresis within the SCS can be designed to drive and localize charged drugs to the posterior pol e, thereby leveraging the combined targeting abilities of iontophoresis and SCS delivery. Since iontophoresis is carried out by ion transfer to the counter electrode as well as the electrical repulsive force of particles, this approach should enable charged drugs to be delivered to the posterior SCS. In addition, highly controlled targeting within the SCS may be possible, by combining the targeting abilities of SCS injection and iontophoresis with high bioavailability at the posterior or anterior segment of SCS. Drug formulations including macromolecules and micro/nanoparticles, which are generally difficult to be delivered by iontophoresis only into the eye, may be delivered by SCS injection, because drugs are injected directly into the SCS by a microneedle without needing to cross epithelial barriers on cornea or conjunctiva. Moreover, since drugs can be delivered into the SCS without penetrating dense ocular layers, delivery to the posterior area by iontophoresis should be faster and more efficient than conventional iontophoresis, even using relatively a small

electric current or voltage. Because iontophoresis and SCS injection have not been combined before, studying drug delivery as well as safety will be important.

Thus, herein, we developed a novel drug delivery system combining SCS injection using a microneedle and iontophoresis in the SCS to test our hypothesis. More specifically, we tested the ability of this approach to target drugs preferentially to sites of action near the posterior pole. In this drug delivery system, a customized Ag/AgCl electrode (for iontophoresis) was embedded into a syringe attached to a microneedle. We used this drug delivery system ex vivo and in vivo to provide a first assessment of delivery and safety of this iontophoretic SCS injection system.

2. Experimental Section

2.1 Device for SCS injection and iontophoresis

For SCS injection, a 1 mL Luer-lock plastic syringe (BD Bioscience, San Jose, CA) was connected to a 30-gauge hollow microneedle measuring 750 μm in length (kindly donated by Clearside Biomedical, Alpharetta, GA) (Fig. 1b). To apply iontophoresis within the SCS, the syringe was modified to contain a disk-type Ag/AgCl electrode with 4 mm diameter and 1 mm thickness (In vivo Metrics, Healdsburg, CA) inside the syringe barrel mounted on the distal end of the syringe plunger (Fig. 1c). A small hole was punctured into the plunger using a gimlet, through which the lead wire from the electrode was fed. The lead wire from this electrode was connected to a power supply (6614C; Agilent Technologies, Santa Clara, CA) to control the electric current. The electric circuit was completed by connecting the power supply to another Ag/AgCl electrode, which was clipped to the rabbit optic nerve (ex vivo, Fig. 1b) or ear (in vivo).

To manage heat and current transfer during iontophoresis, ~500 μL electrolyte gel (Signa gel, Parker Laboratory, Fairfield, NJ) housed in a holder made from polymethyl methacrylate was put around the microneedle (Fig. 1d). The holder measured 8 mm diameter and 6 mm width, and was designed in AutoCAD (Autodesk, San Rafael, CA) and fabricated using a CO_2 laser cutter (VLS3.5, Universal laser system, Scottsdale, AZ).

2.2 Ex Vivo Injection Procedure

Frozen whole New Zealand White rabbit eyes with optic nerve intact (Pel-Freeze, Rogers, AR) were defrosted in a water bath at room temperature (~23°C) for 30 min, and muscles, conjunctiva, and fat around the eyes were removed. To adjust intraocular pressure (IOP) to 10–15 mmHg, Hank's Balanced Salt Solution (HBSS, Mediatech, Manassas, VA) was injected through the inferior sclera into the vitreous, and no leakage was confirmed after the injection. IOP was measured using a tonometer (iCare Tonovet, Helsinki, Finland).

As a model drug formulation, negatively charged red-fluorescent polystyrene nanoparticles with 20 nm diameter (FluoSpheres™, λ_{ex} = 580 nm/ λ_{em} = 605 nm, ζ_{zeta} = −50.9 mV, Life Technologies, Carlsbad, CA) at a concentration of 0.2% w/v in HBSS were filled in the microneedle syringe. The microneedle was inserted perpendicularly into the sclera 3 mm posterior to the limbus at the supranasal position of the ocular globe and 50, 100, or 200 μL of drug formulation was injected into the SCS. Iontophoresis was applied immediately after

injection with the microneedle in place for 1.5, 3, or 5 min at a current of 0, 0.07, 0.14, or 0.7 mA. The counter electrode was attached to the optic nerve.

2.3 In vivo injection procedure

All in vivo procedures were approved by the Georgia Institute of Technology Institutional Animal Care and Use Committee. Practices complied with the ARVO statement for the Use of Animals in Ophthalmic and Vision Research. Albino New Zealand White rabbits (Charles River Breeding Laboratories, Wilmington, MA) were anesthetized by subcutaneous injection of ketamine and xylazine at a dose of 17.5 and 8.5 mg/kg, respectively. Isoflurane gas was used to prolong anesthesia during SCS injection and iontophoresis. Topical anesthesia, proparacaine (Akorn, Lake forest, IL), was applied 3 min prior to SCS injection. To facilitate injection, the eyelid was pushed back and fixed using a latex band. A 100 μL volume of nanoparticle formulation was injected within 3 s into the SCS at a location 3 mm posterior to the limbus at the supranasal location of the ocular globe. Then, iontophoresis was applied at 0.14 mA for 3 min with the microneedle in place and the counter electrode attached to the ear (Fig. S1 in Supplementary Materials).

After iontophoresis, rabbits received an injection of 0.03 mg/kg buprenorphine to reduce the pain after the injection and were monitored for adverse effects for 1 h and then daily for one week. At least three rabbit eyes were used each experimental condition. At the end of the experiment, rabbits were euthanized under the anesthesia with an injection of 150 mg/kg pentobarbital through the ear vein. The eyes were enucleated and analyzed for nanoparticle distribution within the SCS.

2.4 Analysis of nanoparticle distribution in the SCS

To preserve the nanoparticle distribution at the end of each experiment, eyes were immediately frozen in isopropyl alcohol chilled by liquid nitrogen. The fully frozen eyes were dissected by making eight equally spaced radial cuts like flower petals from the posterior pole at the optic nerve to the limbus. The petals were splayed and flattened to expose the chorioretinal surface inside the eye. Bright field images were taken using a digital single-lens reflex camera (Cannon 60d, Melville, NY) to observe nanoparticle distribution. Fluorescence imaging was performed by illuminating the tissue with green LED light (Bluewind Multicolor RGB, HitLight, Baton Rouge, LA) and imaging with an optical bandpass filter (610 ± 10 nm; Edmunds Optics, Barrington, NJ) mounted on the camera.

To quantify nanoparticle spreading in the SCS, the tissue petals were cut to create four segments at 0–3, 3–6, 6–9, and 9- mm from the limbus. These tissue pieces were incubated in radioimmunoprecipitation assay buffer (Abcam, Cambridge, MA) overnight and homogenized to preferentially digest the chorioretinal layer with little effect on the sclera. The supernatant in the solution was transferred to a 96-well plate and relative fluorescence of the extracted nanoparticles was measured by a plate reader (Synergy Microplate Reader, Winooski, VT). Although we did not quantify the efficiency of nanoparticle extraction from tissue, we did not observe significant residual fluorescence in tissue after extraction and all the extraction steps were the same (i.e., any inefficiency was the same in all samples). The average particle distance (APD) was calculated by finding the sum of the center distance

from the limbus of each segment (e.g., the 0–3 mm segment had a center distance of 1.5 mm) weighted by the percent of nanoparticle in that segment.

2.5 Ultrasound measurement of SCS thickness

An ultrasound scanner (UBM Plus, Accutome, Malvern, PA) was used to measure SCS thickness change of the rabbit eye ex vivo. After SCS injection of 50, 100, or 200 μL HBSS at the supranasal location of the ocular globe, ultrasound B scan was performed to measure SCS thickness every minute for 10 min with at least three replicates for each volume.

2.6 Histology

Histological analysis was performed to assess safety of iontophoresis in the SCS using a microneedle. Rabbits treated with SCS injection of HBSS with the iontophoresis were monitored for 1 day or 1 week, and then euthanized. The eyes were enucleated and immediately soaked in 10% formalin solution for 12 h to fix the tissues. The fixed eyes were microtomed to ~10 μm thickness and stained with hematoxylin-eosin (H&E) or periodic acid shiff (PAS). Each sample was imaged to produce cross-sectional views of the tissue around the injection site using a microscope (DP71; Olympus, Tokyo, Japan).

2.7 Statistical Analysis

All data were obtained with at least three replicates, and the mean and standard deviation were calculated. One- and two-way ANOVA with replicates were used for data analysis to estimate the statistical significance of iontophoresis and volume effect. One-way ANOVA with replicates was used for the other analyses, and a p value < 0.05 was considered significant. A p value less than 0.05 was marked with one asterisk (*), and less than 0.01 was marked with two asterisks (**) in the graphs.

3. Result and Discussion

3.1. Device for SCS injection and iontophoresis

We designed a device to enable targeted SCS injection combined with iontophoresis (Fig. 1). The protocol was developed to first inject a solution of charged nanoparticles into the SCS and thereby expand its width and fill it with nanoparticles (Fig. 1a(ii)). While the SCS was still expanded, iontophoresis was applied with a polarity that moved the negatively charged nanoparticles toward the posterior pole (Fig. 1a(iii)).

The system was designed to have a continuous electrical pathway from the electrode located at the base of the syringe plunger (Fig. 1b,c), through HBSS within the syringe and through HBSS in the SCS toward the posterior pole. Ex vivo, the counter electrode was clipped to the optic nerve to facilitate current movement posteriorly. In vivo, the counter electrode was attached to the ear, and the high electrical conductivity of HBSS in the SCS, as well as the inability of the charged nanoparticles to easily flow out of the SCS, directed delivery of nanoparticles toward the posterior pole.

A holder containing electrolyte gel was placed around the microneedle end of the syringe to reduce electrical resistance at the microneedle-tissue interface and to facilitate heat transfer

away from the microneedle-tissue interface, thereby preventing excessive tissue heating during iontophoresis (Fig. 1d).

3.2. Nanoparticle delivery in SCS by iontophoresis

We first tested the hypothesis that iontophoresis can move charged nanoparticles posteriorly in the SCS. Negatively charged fluorescent nanoparticles with 20 nm diameter were injected into the SCS of the rabbit eye ex vivo using a microneedle. Iontophoresis was then applied to drive nanoparticles toward the optic nerve. Enucleating, freezing and dissecting the eye from the posterior pole to the limbus with eight radial cuts produced a flat-mount preparation of the eye looking like flower petals (Fig. 2a, c, e). The center of the "flower" was the site of the cornea, and each "petal" spanned from the limbus to the posterior pole. Nanoparticle distribution in the SCS was quantified by cutting each petal into four pieces and measuring fluorescence of nanoparticles extracted from each piece (Fig. 2b,d,f).

In an eye injected with red-fluorescent nanoparticles, but without application of iontophoresis, nanoparticles were found in the SCS mostly near the limbus, with very few nanoparticles near the posterior pole (Fig. 2a(i) and Fig. 2b). Increasing injection volume from 50 to 200 μl increase nanoparticle delivery posteriorly, but still most particles remained in the anterior SCS (Fig. 2b(i), 2e(i), Fig. 2d,f, and Fig. S2a).

Application of iontophoresis (0.14 mA for 3 min) increased nanoparticle delivery toward the posterior pole. After injection of 50 μL of nanoparticle suspension into the SCS, iontophoresis reduced nanoparticle concentration near the limbus (i.e., 0–3 mm in Fig 2b) and increased nanoparticle concentration 3–6 mm and 6–9 mm away from the limbus toward the posterior pole. However, nanoparticle delivery more than 9 mm from the limbus remained just a few percent both with and without iontophoresis. Increasing injection volume to 100 and 200 μL followed by iontophoresis further increased nanoparticle spreading posteriorly such that up to 31% of nanoparticles reached the most posterior portion of the SCS (i.e., >9 mm from the limbus) (Fig. S2b).

Because the fluorescence images (Fig 2a, Fig 2c and Fig 2e) only show the two-dimensional distribution of particles in the SCS, they mostly show the presence of particles but do not easily show concentration of particles through the SCS thickness. We therefore believe that the graphs (Fig 2b, Fig 2d and Fig 2f) provide better quantitative information.

As another measure of iontophoresis driving charged nanoparticles posteriorly, the average particle distance from the limbus (i.e., APD) was determined, and was found to be significantly greater after iontophoresis (i.e., > 6 mm from the limbus) than after SCS injection alone (Fig. 2g). Thus, application of iontophoresis and increasing SCS injection volume both increased nanoparticle delivery toward back of the eye.

3.3. Effect of iontophoresis current

To determine the effect of current intensity, iontophoresis was applied at 0, 0.14 and 0.7 mA for 3 min after SCS injection (200 μL) of nanoparticles. The nanoparticle distribution shifted more posteriorly with increasing current, which is consistent with the expected mechanism of current-driven transport of the charged nanoparticles (Fig. 3b,c). Although iontophoresis

at 0.7 mA showed the best result, the difference in posterior delivery compared to iontophoresis at 0.14 mA was relatively small.

Examination of the fluorescent micrographs may explain why (Fig. 3a). In the absence of iontophoresis, the petals containing red-fluorescent nanoparticles shown a relatively even coloring as a function of position (Fig. 3a(i)). Iontophoresis at 0.14 mA resulted in the petals near the injection site having even coloring, but the more-distant petals showing mottled coloring (Fig. 3a(ii)). At 0.7 mA, mottled coloring was increased in the outer petals and began to appear in the petals near the injection site as well (Fig. 3a(iii)). These observations suggest that iontophoresis focuses nanoparticle transport from the injection site to the posterior pole with less movement to the sides and that this focusing is increased at higher current.

We interpret the mottled appearance of fluorescence in some images as evidence of nanoparticle aggregation in the SCS (see also Fig S3). Since iontophoresis is carried out by ion transfer to the counter electrode as well as the electrical repulsive force of particles, iontophoresis not only delivers the particles to the posterior direction but increases the chance of interaction among ions and particles, inducing charge non-uniformity (neutralizing particle charge). Due to the charge non-uniformity of the particles, we believe that aggregation occurred. In particular, at higher current, aggregation is increased [51–53].

Although 0.7 mA provided better posterior delivery, we selected 0.14 mA as the preferred current in the interest of safety. High current density can cause tissue damage [35, 54], so we opted for the lower current, which provided almost as good posterior transport.

3.4. Effect of iontophoresis application time

Since iontophoresis application time is expected to affect delivery to the posterior eye, iontophoresis was performed for different application times. As application time increased from 1.5 to 3 min, more nanoparticles were delivered posteriorly (i.e., ~30% delivered >9 mm from the limbus, Fig. 4b) and the average particle distance increase as well (i.e., ~6 mm from the limbus, Fig. 4c), which was expected. However, increasing application time from 3 to 5 min did not improve posterior delivery, i.e., the percentage of nanoparticles delivered >9 mm from the limbus was decreased (Fig. 4b) and the average particle distance was unchanged (Fig. 4c), which was not expected. Closer examination of the images of nanoparticle distribution in the SCS shows a mottled appearance of fluorescence (Fig. 4a) like that seen at high current (Fig. 3a), which suggest that long application times may cause nanoparticle aggregation, which could at least partially explain the reduced effectiveness of increasing iontophoresis application time beyond 3 min.

Another possible explanation could be that the SCS rapidly collapses after injection. In previous studies, the SCS collapse time in rabbit eyes in vivo (after injection of 50 μL HBSS buffer) was reported around 40 min [55, 56], which is much longer than the 3 – 5 min timeframe of iontophoresis in this study. However, the SCS of the rabbit eye ex vivo may collapse much faster than in vivo. To assess this possibility, SCS collapse time of the rabbit eye ex vivo was measured using B-scan ultrasound imaging. After SCS injection with 50, 100, and 200 μL of HBSS containing nanoparticles, SCS thickness was measured every

minute for 10 min at the injection site (Fig. 5, Fig. S4). At all three injection volumes SCS thickness was around 1 mm immediately after injection. After 1 min, SCS thickness decreased by at least 50% (Fig. 5). After 3 min, the SCS still appeared to be partially open (Fig. S4), but after 5 min, the SCS generally appeared to be completely collapsed in all three cases (Fig. 5(iii)). This rapid collapse within 5 min may have interfered with nanoparticle movement toward the posterior pole. The observation that SCS collapse time was independent of injection volume between 50 – 200 μL may be explained by the larger area of spread in the SCS thickness at higher injection volume [56], which may enable more rapid resorption of fluid from the SCS at larger injection volume.

3.5. Effect of iontophoresis polarity

The direction of iontophoretic movement of charged particles should be determined largely by the direction of the iontophoresis. Thus, switching iontophoresis polarity should generate iontophoretic forces that keep nanoparticles at the injection site near the limbus. The data support this expectation, where iontophoresis with reversed polarity kept nanoparticles close to the site of injection and led to a nanoparticle distribution in the SCS that was more anterior than injection without iontophoresis (Fig. 6).

3.6. In vivo nanoparticle delivery by iontophoresis

Based on the ex vivo results, nanoparticle delivery by iontophoresis was studied in the rabbit eye in vivo using 100 μL injection of nanoparticles followed by iontophoresis at 0.14 mA for 3 min. Although increasing injection volume (up to 200 μL) increased posterior targeting, SCS injection using volumes as large as 200 μL have not been extensively studied in vivo and have uncertain safety profile. Standard SCS injections, and intravitreal injections, in humans are just 50 μL [57]. Prior studies in New Zealand white rabbits have found that injection of 50–100 μL into the SCS was well tolerated [30, 34, 58]. Thus, we chose 100 μL injection volume for in vivo experiments.

After injection without iontophoresis, nanoparticles were spread in the SCS similarly to findings after injection in the rabbit eye ex vivo (Fig. 7a(i)). Since prior studies in New Zealand white rabbits using similar nanoparticles injected into the SCS showed that particle fluorescence distribution was similar between 0 days and 14 days after injection, we did not assess particle distribution over time after the injection without iontophoresis [30]. Examination of images taken 1 hour after iontophoresis shows petals near the injection site with fluorescent nanoparticles throughout the petals from the limbus to the posterior pole (Fig. 7a(ii)). Other petals located distant to the injection site show nanoparticles localized only near the posterior pole with little or no nanoparticles near the limbus (Fig. 7a(ii)). To explain this nanoparticle distribution, it appears that nanoparticles at the posterior end of the petals were delivered from petals in the opposite side of the eye by iontophoresis around the optic nerve (Fig. S5).

This delivery pattern imaged 1 h after iontophoresis resulted in ~30% of nanoparticles delivered >9 mm from the limbus (Fig. 7b(ii)), and the average position of nanoparticles ~6 mm from the limbus (Fig. 7c(ii)), in good agreement with findings ex vivo. Examination of

nanoparticles in the SCS 1 week after iontophoresis showed a similar distribution (Fig. 7b(iii)) and average distance from the limbus (Fig. 7c(iii)) compared to findings at 1 h.

3.7. In vivo safety analysis

The safety of iontophoresis in the SCS was assessed by clinical exam and histology. After iontophoresis, the injection site was observed with the naked eye. Tissue at the injection site appeared normal, with no evidence of tissue damage, inflammation, or burns (Fig. S6). No adverse events were reported by the veterinarian staff caring for the rabbits at any time. Safety of the procedure may have been enhanced by iontophoresis device design. Since the electric current can generate heat around the electrode in the syringe during iontophoresis, a thermally (and electrically) conductive electrolyte gel was placed in the microneedle holder to dissipate heat from the microneedle and surrounding tissue.

Histological analysis was performed to further examine effects of iontophoresis on tissue around the injection site (Fig. S7). Tissue was collected one day after iontophoresis from three different rabbits. Tissue from one rabbit eye appeared normal (Fig. S7b(i)). However, evidence of mild choroidal inflammation was seen in the second rabbit (Fig. S7b(ii)) and minor chorioretinal “scarring” was seen in the third rabbit (Fig. S7b(iii)) near the site of injection. We do not have histology from eyes that received SCS injection without iontophoresis, so we do not know the role of SCS injection versus iontophoresis in generating these effects. However, prior studies have not usually shown tissue damage from SCS injection [16, 34, 59], so we believe that iontophoresis is more likely the cause.

One week after iontophoresis, eyes from three additional rabbits were examined histologically and all three appeared normal (Fig. S7c). This indicates that although iontophoresis in the SCS may generate minor tissue damage at the site of injection, the tissue can recover within 1 week. The effects of repeated injection, which may be needed to treat chronic diseases was not assessed here and will require future studies. However, these findings are based on limited data collected at just one iontophoresis condition in rabbits. Thus, safety issues should be further studied and optimized by possible modification of electrode design, iontophoresis conditions and other factors.

3.8. Study limitations

The experimental set-ups in the ex vivo and in vivo studies were different, making direct comparisons difficult. We used the ex vivo set-up to study the effects of iontophoretic parameters on nanoparticle delivery in the SCS. While these ex vivo findings will not translate directly to the in vivo environment, we believe that the principles shown in the ex vivo study can nonetheless be used to guide and interpret findings in vivo. Thus, we optimized iontophoresis parameters ex vivo to guide the parameters used in this first study of SCS iontophoresis in vivo.

The microneedle injection method and microneedle electrode were used in the same way in the ex vivo and in vivo studies. Previous iontophoresis studies in vivo (using New Zealand white rabbits) attached the counter electrode to the rabbit ear for drug delivery to the back of the eye [36, 60]. However, since there is no ear in the ex vivo study, we attached the counter electrode to the optic nerve instead.

While transport of nanoparticles in the SCS by iontophoresis can be more easily studied ex vivo, understanding safety concerns requires in vivo study. In ex vivo experiments, we looked for direct effects of iontophoresis on tissue structures, but issues of cell death, inflammation and other responses were only considered in vivo. The gross observation and histological analysis performed in this study in vivo provides an initial as sessment of safety, but additional studies are needed, especially to assess long-term effects and the effects of possible repeated administration to treat chronic conditions.

In principle, charged drugs can be delivered by iontophoresis regardless of negative or positive charge by adjusting the electric field polarity. However, drug – tissue interactions may be influenced by charge, where positively charged drugs may more likely bind to negatively charged tissue [2, 61, 62]. Delivery of DNA, RNA and other highly charged compounds would be most suitable for delivery using iontophoresis. In contrast, weakly charged drugs (e.g. bevacizumab and ranibizumab) may be delivered less efficiently by iontophoresis. However, this limitation can be addressed by drug formulation modification, such as conjugation with highly charged polymer or encapsulation in charged particles or liposomes, to generate strong charge around the drug. Future studies will be needed to build off this initial study of iontophoresis in the SCS and more fully assess its strengths and weaknesses.

4. Conclusion

In this study, iontophoresis in the SCS using a microneedle for targeted drug delivery in the eye was studied for the first time. We first designed a device comprised of a hollow microneedle attached to a syringe to enable targeted injection into the SCS, an electrode embedded to the syringe to administer iontophoresis into the SCS (in combination with a counter-electrode attached to the optic nerve ex vivo or to the rabbit ear in vivo), and a holder containing electrolyte gel placed around the microneedle to increase electrical and thermal conductivity at the microneedle-tissue interface.

When charged nanoparticles were injected into the SCS, the application of iontophoresis increased the transport of nanoparticles posteriorly toward the posterior pole. Increasing injection volume (between 50 and 200 μL) increased posterior targeting of nanoparticle delivery. Increasing iontophoresis current from 0.14 to 0.7 mA led to a small increase in posterior targeting, but concern about possible tissue damage from the higher current led us to prefer the lower current as a safer option. Increasing iontophoresis application time from 1.5 to 3 min increased posterior targeting, but further increasing to 5 min did not help. Ultrasound imaging showed that the SCS of the rabbit eye ex vivo collapsed within ~5 min, which may explain why additional nanoparticle transport did not occur between 3 and 5 min.

Based on the findings from ex vivo studies, we carried out SCS iontophoresis in the rabbit eye in vivo using 100 μL injection of nanoparticles followed by iontophoresis at 0.14 mA for 3 min. At these conditions, approximately 30% of charged nanoparticles were localized in the most posterior region of the SCS (>9 mm from the limbus) and the average nanoparticle distance from the SCS was approximately 6 mm. These findings are in good agreement with

ex vivo data. Iontophoresis in the SCS was generally well tolerated, with only mild, transient tissue effects at the site of injection.

We conclude that iontophoresis can increase posterior targeting of charged nanoparticles in the SCS after injection using a microneedle. Future treatment of ocular indications, especially those located toward the posterior pole, could benefit from ocular drug delivery targeted by iontophoresis in the SCS

Supplementary Material

Refer to Web version on PubMed Central for supplementary material.

Acknowledgments

We thank Donna Bondy for administrative support. This work was supported by the National Institutes of Health [R01 EY022097]. Mark Prausnitz is an inventor of patents licensed to companies developing microneedle-based products, is a paid advisor to companies developing microneedle-based products, and is a founder/shareholder of companies developing microneedle-based products (Clearside Biomedical). This potential conflict of interest has been disclosed and is managed by Georgia Tech and Emory University.

References

1. Kim YC, Chiang B, Wu X, Prausnitz MR. Ocular delivery of macromolecules. J Control Release. 2014; 190:172–181. [PubMed: 24998941]
2. Patel A, Cholkar K, Agrahari V, Mitra AK. Ocular drug delivery systems: An overview. World J Pharmacol. 2013; 2:47–64. [PubMed: 25590022]
3. Kang-Mieler JJ, Osswald CR, Mieler WF. Advances in ocular drug delivery: emphasis on the posterior segment. Expert Opinion on Drug Delivery. 2014; 11:1647–1660. [PubMed: 24975820]
4. Pearce W, Hsu J, Yeh S. Advances in drug delivery to the posterior segment. Curr Opin Ophthalmol. 2015; 26:233–239. [PubMed: 25759965]
5. Syed BA, Evans JB, Bielory L. Wet AMD market. Nat Rev Drug Discov. 2012; 11:827. [PubMed: 23080338]
6. Holz FG, Schmitz-Valckenberg S, Fleckenstein M. Recent developments in the treatment of age-related macular degeneration. J Clin Invest. 2014; 124:1430–1438. [PubMed: 24691477]
7. Rowe-Rendleman CL, Durazo SA, Kompella UB, Rittenhouse KD, Di Polo A, Weiner AL, Grossniklaus HE, Naash MI, Lewin AS, Horsager A, Edelhauser HF. Drug and gene delivery to the back of the eye: from bench to bedside. Invest Ophthalmol Vis Sci. 2014; 55:2714–2730. [PubMed: 24777644]
8. Falavarjani KG, Nguyen QD. Adverse events and complications associated with intravitreal injection of anti-VEGF agents: a review of literature. Eye (Lond). 2013; 27:787–794. [PubMed: 23722722]
9. Moisseiev E, Loewenstein A, Yiu G. The suprachoroidal space: from potential space to a space with potential. Clin Ophthalmol. 2016; 10:173–178. [PubMed: 26869750]
10. Rai Udo J, Young SA, Thrimawithana TR, Abdelkader H, Alani AW, Pierscionek B, Alany RG. The suprachoroidal pathway: a new drug delivery route to the back of the eye. Drug Discov Today. 2015; 20:491–495. [PubMed: 25448755]
11. Olsen TW, Feng X, Wabner K, Conston SR, Sierra DH, Folden DV, Smith ME, Cameron JD. Cannulation of the suprachoroidal space: a novel drug delivery methodology to the posterior segment. Am J Ophthalmol. 2006; 142:777–787. [PubMed: 16989764]
12. Kadam RS, Williams J, Tyagi P, Edelhauser HF, Kompella UB. Suprachoroidal delivery in a rabbit ex vivo eye model: influence of drug properties, regional differences in delivery, and comparison with intravitreal and intracameral routes. Mol Vis. 2013; 19:1198–1210. [PubMed: 23734089]

13. El Rayes EN, Oshima Y. Suprachoroidal buckling for retinal detachment. Retina. 2013; 33:1073–1075. [PubMed: 23612022]
14. El Rayes EN. Supra choroidal buckling in managing myopic vitreoretinal interface disorders: 1-year data. Retina. 2014; 34:129–135. [PubMed: 23615349]
15. Del Amo EM, Rimpela AK, Heikkinen E, Kari OK, Ramsay E, Lajunen T, Schmitt M, Pelkonen L, Bhattacharya M, Richardson D, Subrizi A, Turunen T, Reinisalo M, Itkonen J, Toropainen E, Casteleijn M, Kidron H, Antopolsky M, Vellonen KS, Ruponen M, Urtti A. Pharmacokinetic aspects of retinal drug delivery. Prog Retin Eye Res. 2017; 57:134–185. [PubMed: 28028001]
16. Gilger BC, Abarca EM, Salmon JH, Patel S. Treatment of acute posterior uveitis in a porcine model by injection of triamcinolone acetonide into the suprachoroidal space using microneedles. Invest Ophthalmol Vis Sci. 2013; 54:2483–2492. [PubMed: 23532526]
17. Patel SR, Berezovsky DE, McCarey BE, Zarnitsyn V, Edelhauser HF, Prausnitz MR. Targeted administration into the suprachoroidal space using a microneedle for drug delivery to the posterior segment of the eye. Invest Ophthalmol Vis Sci. 2012; 53:4433–4441. [PubMed: 22669719]
18. Patel SR, Lin AS, Edelhauser HF, Prausnitz MR. Suprachoroidal drug delivery to the back of the eye using hollow microneedles. Pharm Res. 2011; 28:166–176. [PubMed: 20857178]
19. Kim YC, Edelhauser HF, Prausnitz MR. Particle-stabilized emulsion droplets for gravity-mediated targeting in the posterior segment of the eye. Adv Healthc Mater. 2014; 3:1272–1282. [PubMed: 24652782]
20. Patel SR, Prausnitz MR. Targeted Drug Delivery Within the Eye Through the Suprachoroidal Space. J Ocul Pharmacol Ther. 2016; 32:640–641. [PubMed: 27849435]
21. Einmahl S, Savoldelli M, D'Hermies F, Tabatabay C, Gurny R, Behar-Cohen F. Evaluation of a novel biomaterial in the suprachoroidal space of the rabbit eye. Invest Ophthalmol Vis Sci. 2002; 43:1533–1539. [PubMed: 11980871]
22. Hou J, Tao Y, Jiang YR, Wang K. In vivo and in vitro study of suprachoroidal fibrin glue. Jpn J Ophthalmol. 2009; 53:640–647. [PubMed: 20020245]
23. Kim SH, Galban CJ, Lutz RJ, Dedrick RL, Csaky KG, Lizak MJ, Wang NS, Tansey G, Robinson MR. Assessment of subconjunctival and intrascleral drug delivery to the posterior segment using dynamic contrast-enhanced magnetic resonance imaging. Invest Ophthalmol Vis Sci. 2007; 48:808–814. [PubMed: 17251481]
24. Tyagi P, Kadam RS, Kompella UB. Comparison of suprachoroidal drug delivery with subconjunctival and intravitreal routes using noninvasive fluorophotometry. PLoS One. 2012; 7:e48188. [PubMed: 23118950]
25. Wang M, Liu W, Lu Q, Zeng H, Liu S, Yue Y, Cheng H, Liu Y, Xue M. Pharmacokinetic comparison of ketorolac after intracameral, intravitreal, and suprachoroidal administration in rabbits. Retina. 2012; 32:2158–2164. [PubMed: 23099451]
26. Goldstein DA, Do D, Noronha G, Kissner JM, Srivastava SK, Nguyen QD. Suprachoroidal Corticosteroid Administration: A Novel Route for Local Treatment of Noninfectious Uveitis. Transl Vis Sci Technol. 2016; 5:14.
27. ClinicalTrials.gov. Suprachoroidal Injection of CLS-TA in Subjects With Macular Edema Associated With Non-infectious Uveitis (PEACHTREE). 2017. pp. NCT02595398
28. ClinicalTrials.gov. Triamcinolone Acetonide With IVT Aflibercept in Subjects With Macular Edema Following RVO (SAPPHIRE). 2017. pp. NCT02980874
29. ClinicalTrials.gov. Suprachoroidal Injection of CLS-TA Alone or With Aflibercept in Subjects With Diabetic Macular Edema (HULK). 2017. pp. NCT02949024
30. Kim YC, Oh KH, Edelhauser HF, Prausnitz MR. Formulation to target delivery to the ciliary body and choroid via the suprachoroidal space of the eye using microneedles. Eur J Pharm Biopharm. 2015; 95:398–406. [PubMed: 26036448]
31. Patel AK, Zambarakji HJ, Charteris DG, Sullivan PM. Suprachoroidal silicone oil: recognition and possible mechanisms. Eye (Lond). 2006; 20:854–856. [PubMed: 16113640]
32. Chiang B, Kim YC, Edelhauser HF, Prausnitz MR. Circumferential flow of particles in the suprachoroidal space is impeded by the posterior ciliary arteries. Exp Eye Res. 2016; 145:424–431. [PubMed: 26976663]

33. Chiang B, Venugopal N, Edelhauser HF, Prausnitz MR. Distribution of particles, small molecules and polymeric formulation excipients in the suprachoroidal space after microneedle injection. Exp Eye Res. 2016; 153:101–109. [PubMed: 27742547]
34. Chiang B, Kim YC, Doty AC, Grossniklaus HE, Schwendeman SP, Prausnitz MR. Sustained reduction of intraocular pressure by supraciliary delivery of brimonidine-loaded poly(lactic acid) microspheres for the treatment of glaucoma. J Control Release. 2016; 228:48–57. [PubMed: 26930266]
35. Eljarrat-Binstock E, Domb AJ. Iontophoresis: a non-invasive ocular drug delivery. J Control Release. 2006; 110:479–489. [PubMed: 16343678]
36. Eljarrat-Binstock E, Orucov F, Aldouby Y, Frucht-Pery J, Domb AJ. Charged nanoparticles delivery to the eye using hydrogel iontophoresis. J Control Release. 2008; 126:156–161. [PubMed: 18201790]
37. Vollmer DL, Szlek MA, Kolb K, Lloyd LB, Parkinson TM. In vivo transscleral iontophoresis of amikacin to rabbit eyes. J Ocul Pharmacol Ther. 2002; 18:549–558. [PubMed: 12537681]
38. Barza M, Peckman C, Baum J. Transscleral iontophoresis of cefazolin, ticarcillin, and gentamicin in the rabbit. Ophthalmology. 1986; 93:133–139. [PubMed: 3951811]
39. Behar-Cohen FF, El Aouni A, Gautier S, David G, Davis J, Chapon P, Parel JM. Transscleral Coulomb-controlled iontophoresis of methylprednisolone into the rabbit eye: influence of duration of treatment, current intensity and drug concentration on ocular tissue and fluid levels. Exp Eye Res. 2002; 74:51–59. [PubMed: 11878818]
40. Eljarrat-Binstock E, Raiskup F, Frucht-Pery J, Domb AJ. Transcorneal and transscleral iontophoresis of dexamethasone phosphate using drug loaded hydrogel. J Control Release. 2005; 106:386–390. [PubMed: 16026884]
41. Eljarrat-Binstock E, Raiskup F, Frucht-Pery J, Domb AJ. Hydrogel probe for iontophoresis drug delivery to the eye. J Biomater Sci Polym Ed. 2004; 15:397–413. [PubMed: 15212325]
42. Voigt M, Kralinger M, Kieselbach G, Chapon P, Anagnoste S, Hayden B, Parel JM. Ocular aspirin distribution: a comparison of intravenous, topical, and coulomb-controlled iontophoresis administration. Invest Ophthalmol Vis Sci. 2002; 43:3299–3306. [PubMed: 12356838]
43. Myles ME, Neumann DM, Hill JM. Recent progress in ocular drug delivery for posterior segment disease: emphasis on transscleral iontophoresis. Adv Drug Deliv Rev. 2005; 57:2063–2079. [PubMed: 16310884]
44. Gungor S, Delgado-Charro MB, Ruiz-Perez B, Schubert W, Isom P, Moslemy P, Patane MA, Guy RH. Trans-scleral iontophoretic delivery of low molecular weight therapeutics. J Control Release. 2010; 147:225–231. [PubMed: 20655965]
45. Erlanger G. Iontophoresis, a scientific and practical tool in ophthalmology. Ophthalmologica. 1954; 128:232–246. [PubMed: 13224179]
46. Hughes L, Maurice DM. A fresh look at iontophoresis. Arch Ophthalmol. 1984; 102:1825–1829. [PubMed: 6508622]
47. Sarraf D, Lee DA. The role of iontophoresis in ocular drug delivery. J Ocul Pharmacol. 1994; 10:69–81. [PubMed: 8207346]
48. Ghate D, Edelhauser HF. Barriers to glaucoma drug delivery. J Glaucoma. 2008; 17:147–156. [PubMed: 18344762]
49. Huang AJ, Tseng SC, Kenyon KR. Paracellular permeability of corneal and conjunctival epithelia. Invest Ophthalmol Vis Sci. 1989; 30:684–689. [PubMed: 2703309]
50. Nakao S, Hafezi-Moghadam A, Ishibashi T. Lymphatics and lymphangiogenesis in the eye. J Ophthalmol. 2012; 2012:783163. [PubMed: 22523652]
51. Lebovka NI. Aggregation of Charged Colloidal Particles. Adv Polym Sci. 2014; 255:57–96.
52. Kloepper KD, Onuta TD, Amarie D, Dragnea B. Field-induced interfacial properties of gold nanoparticles in AC microelectrophoretic experiments. Journal of Physical Chemistry B. 2004; 108:2547–2553.
53. Rajnak M, Petrenko VI, Avdeev MV, Ivankov OI, Feoktystov A, Dolnik B, Kurimsky J, Kopcansky P, Timko M. Direct observation of electric field induced pattern formation and particle aggregation in ferrofluids. Appl Phys Lett. 2015; 107

54. Gurny R, Kaltsatos VV, Deshpande AA, Zignani M, Percicot C, Baeyens VV. Ocular drug delivery in veterinary medicine. Adv Drug Deliv Rev. 1997; 28:335–361. [PubMed: 10837574]

55. Chiang B, Wang K, Ethier CR, Prausnitz MR. Clearance Kinetics and Clearance Routes of Molecules From the Suprachoroidal Space After Microneedle Injection. Invest Ophthalmol Vis Sci. 2017; 58:545–554. [PubMed: 28125841]

56. Chiang B, Venugopal N, Grossniklaus HE, Jung JH, Edelhauser HF, Prausnitz MR. Thickness and Closure Kinetics of the Suprachoroidal Space Following Microneedle Injection of Liquid Formulations. Invest Ophthalmol Vis Sci. 2017; 58:555–564. [PubMed: 28125842]

57. Peyman GA, Lad EM, Moshfeghi DM. Intravitreal injection of therapeutic agents. Retina. 2009; 29:875–912. [PubMed: 19584648]

58. Chen M, Li XL, Liu JK, Han Y, Cheng LY. Safety and pharmacodynamics of suprachoroidal injection of triamcinolone acetonide as a controlled ocular drug release model. Journal of Controlled Release. 2015; 203:109–117. [PubMed: 25700623]

59. Kim YC, Edelhauser HF, Prausnitz MR. Targeted delivery of antiglaucoma drugs to the supraciliary space using microneedles. Invest Ophthalmol Vis Sci. 2014; 55:7387–7397. [PubMed: 25212782]

60. Souza JG, Dias K, Silva SA, de Rezende LC, Rocha EM, Emery FS, Lopez RF. Transcorneal iontophoresis of dendrimers: PAMAM corneal penetration and dexamethasone delivery. J Control Release. 2015; 200:115–124. [PubMed: 25553828]

61. Gaudana R, Ananthula HK, Parenky A, Mitra AK. Ocular drug delivery. AAPS J. 2010; 12:348–360. [PubMed: 20437123]

62. Kim SH, Lutz RJ, Wang NS, Robinson MR. Transport barriers in transscleral drug delivery for retinal diseases. Ophthalmic Res. 2007; 39:244–254. [PubMed: 17851264]

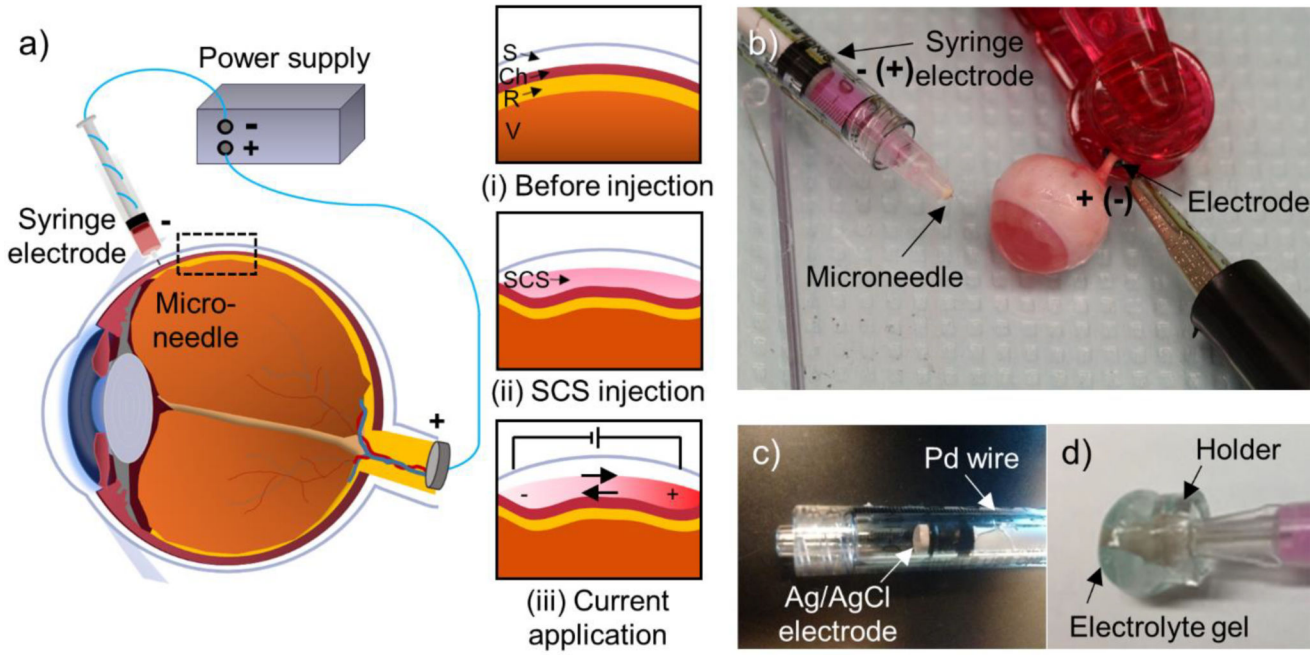

Figure 1.

Drug delivery targeted by iontophoresis in the suprachoroidal space (SCS) of the eye. a) Schematic illustration of iontophoretic targeting of ocular drug delivery via the SCS. Targeting (i) the space between sclera and choroid (ii) opens the SCS to fill it with injected drug formulation, after which (iii) iontophoresis is used to move charged species within the SCS. b) The device for SCS injection and iontophoresis comprises a syringe containing an electrode for iontophoresis and a microneedle for injection. The counter electrode is attached to the optic nerve of a rabbit eye ex vivo. c) The electrode in the syringe is mounted on the distal end of the syringe plunger. d) A holder with electrolyte gel can be added to provide increased electrical conductivity that improves electrical connectivity between the microneedle device and ocular tissue and to provide increased thermal conductivity to protect ocular tissue by conducting heat away from the microneedle and tissue.

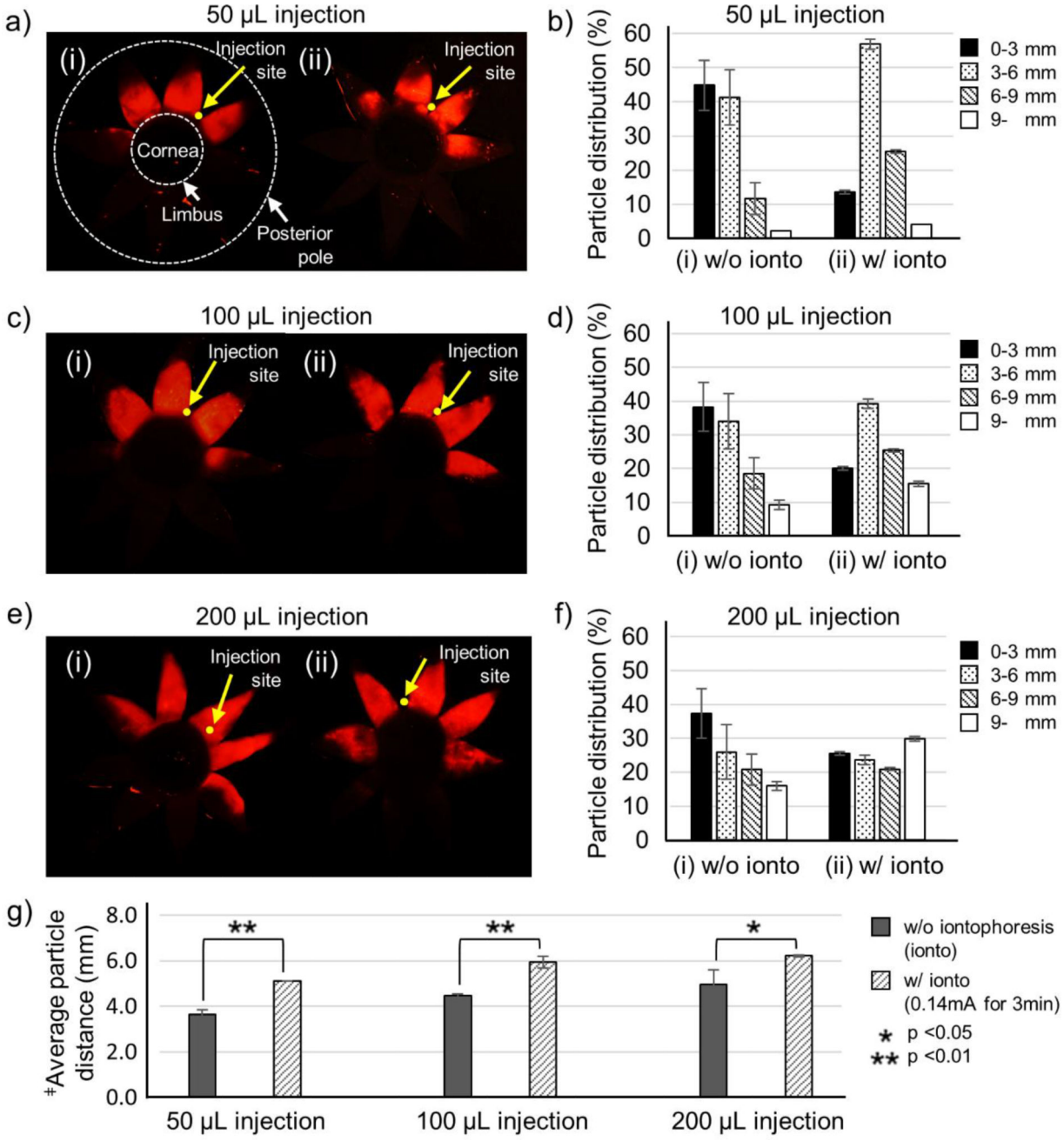

Figure 2.

Effect of the iontophoretic targeting within the suprachoroidal space (SCS) at different SCS injection volumes. Representative fluorescence micrographs (a, c, e) and distributions of red-fluorescent nanoparticles in the SCS (b, d, f) after injection of nanoparticles in HBSS into the SCS of rabbit eyes ex vivo (i) without iontophoresis and (ii) with iontophoresis at 0.14 mA for 3 min. SCS injection volumes were 50 µL (a, b), 100 µL (c, d) and 150 µL (e, f). Fluorescence micrographs (a, c, e) show representative flat mounts of the eye after dissection with radial cuts from the posterior pole to the limbus to form 8 “petals.” Yellow arrows point to sites of injection into the SCS. The cornea is located in the center of the

petals, and the posterior pole is at the tips of the petals. Two white dashed lines indicate the location of the limbus and the posterior pole. Average distance of nanoparticle transfer (g) was calculated based on the nanoparticle distribution. ‡Average particle distance (APD) (mm) = (1.5 mm × % of nanoparticles in 0–3 mm area) + (4.5 mm × % of nanoparticles in 3–6 mm area) + (7.5 mm × % of nanoparticles in 6–9 mm area) + (10.5 mm × % of nanoparticles in 9- mm area). Graphs (b, d, f, g) present average ± standard deviation based on 3 replicate samples.

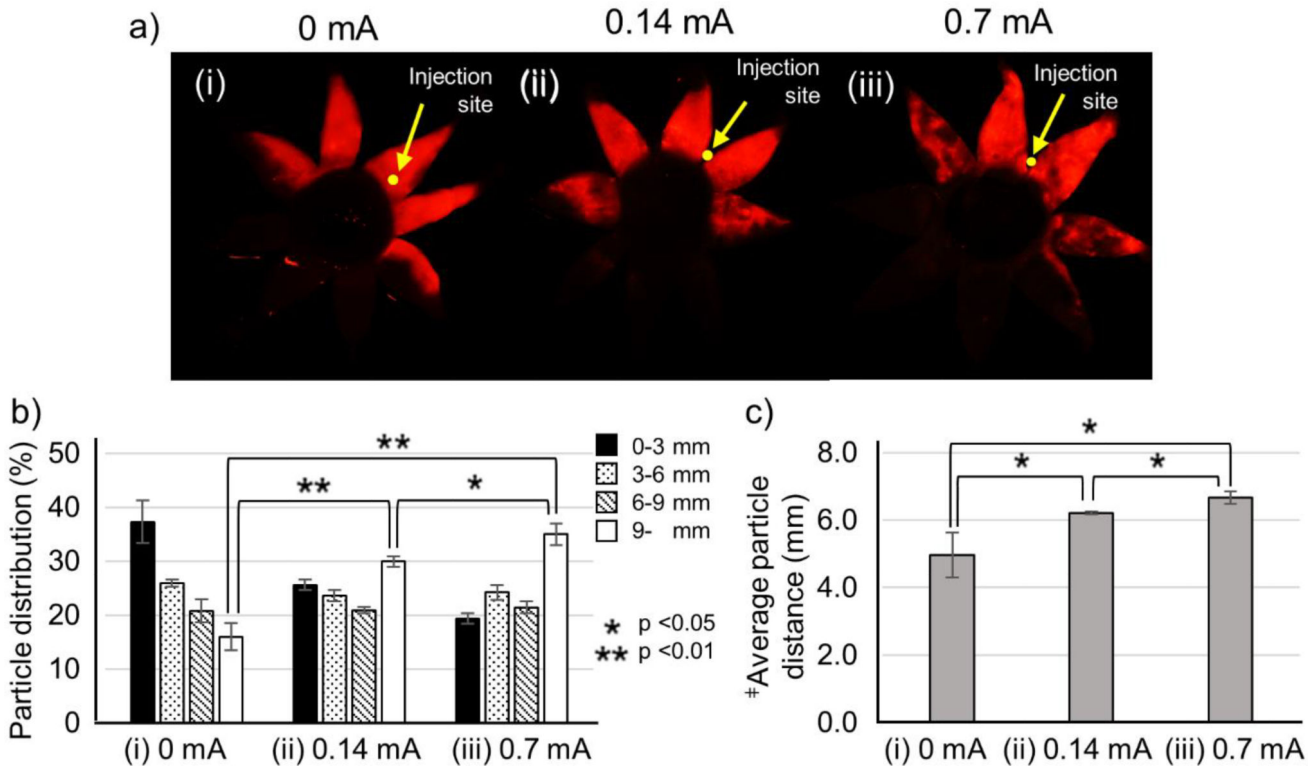

Figure 3.

Effect of the iontophoresis current applied after of injection of nanoparticles in the suprachoroidal space (SCS). Representative fluorescence micrographs (a), distribution of red-fluorescent nanoparticles in the SCS (b) and average distance of nanoparticle transfer in the SCS (c) (i) without iontophoresis (0 mA) and with iontophoresis at (ii) 0.14 mA and (iii) 0.7 mA for 3 min after injection of 200 μL of nanoparticles in HBSS into the SCS of rabbit eyes ex vivo. Fluorescence micrographs (a) show representative flat mounts of the eye after dissection with radial cuts from the posterior pole to the limbus to form 8 “petals.” Yellow arrows point to sites of injection into the SCS. ‡Average particle distance (APD) (mm). Graphs (b and c) present average ± standard deviation based on 3 replicate samples.

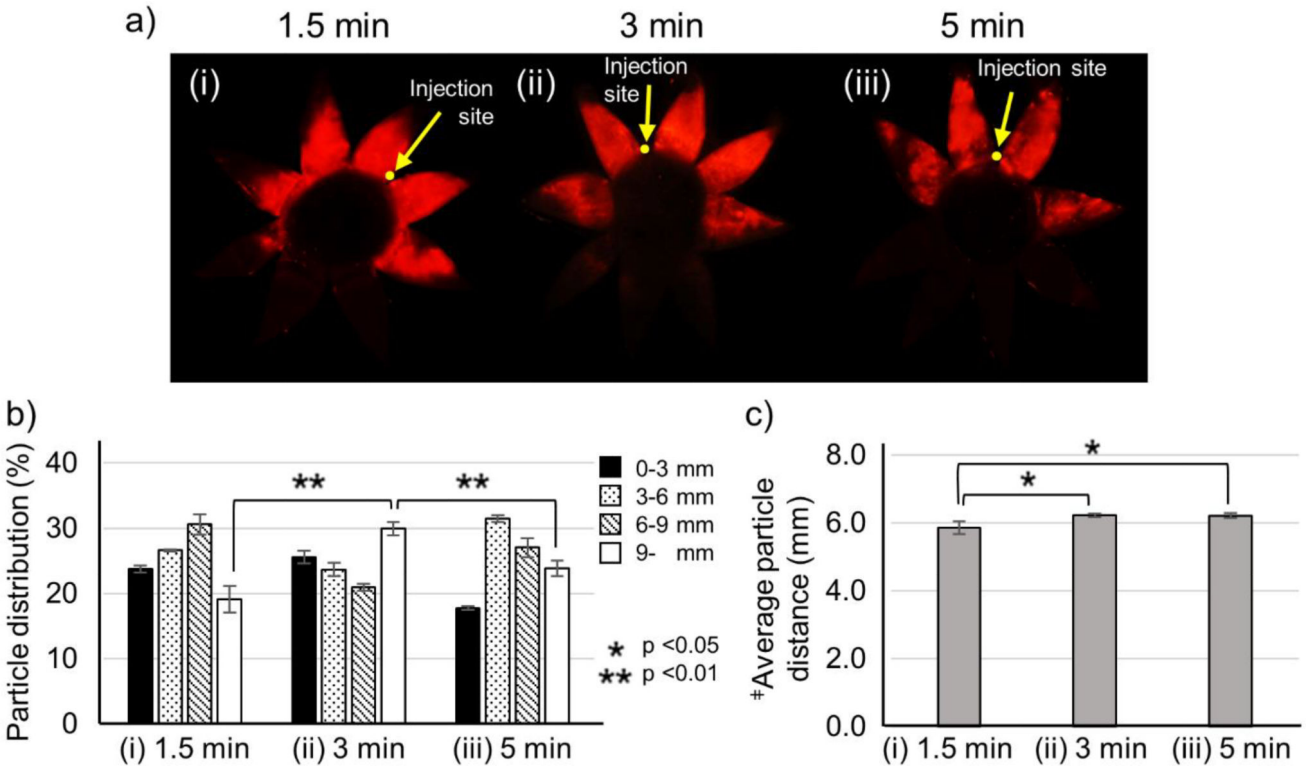

Figure 4.

Effect of iontophoresis application time after injection of nanoparticles in the suprachoroidal space (SCS). Representative fluorescence micrographs (a), distribution of red-fluorescent nanoparticles in the SCS (b), average distance of nanoparticle transfer in the SCS (c) due to iontophoresis at 0.14 mA for (i) 1.5 min, (ii) 3 min, and (iii) 5 min after injection of 200 μL of nanoparticles in HBSS into the SCS of rabbit eyes ex vivo. Fluorescence micrographs (a) show representative flat mounts of the eye after dissection with radial cuts from the posterior pole to the limbus. Yellow arrows point to sites of injection into the SCS. ‡Average particle distance (APD) (mm). Graphs (b and c) present average ± standard deviation based on 3 replicate samples.

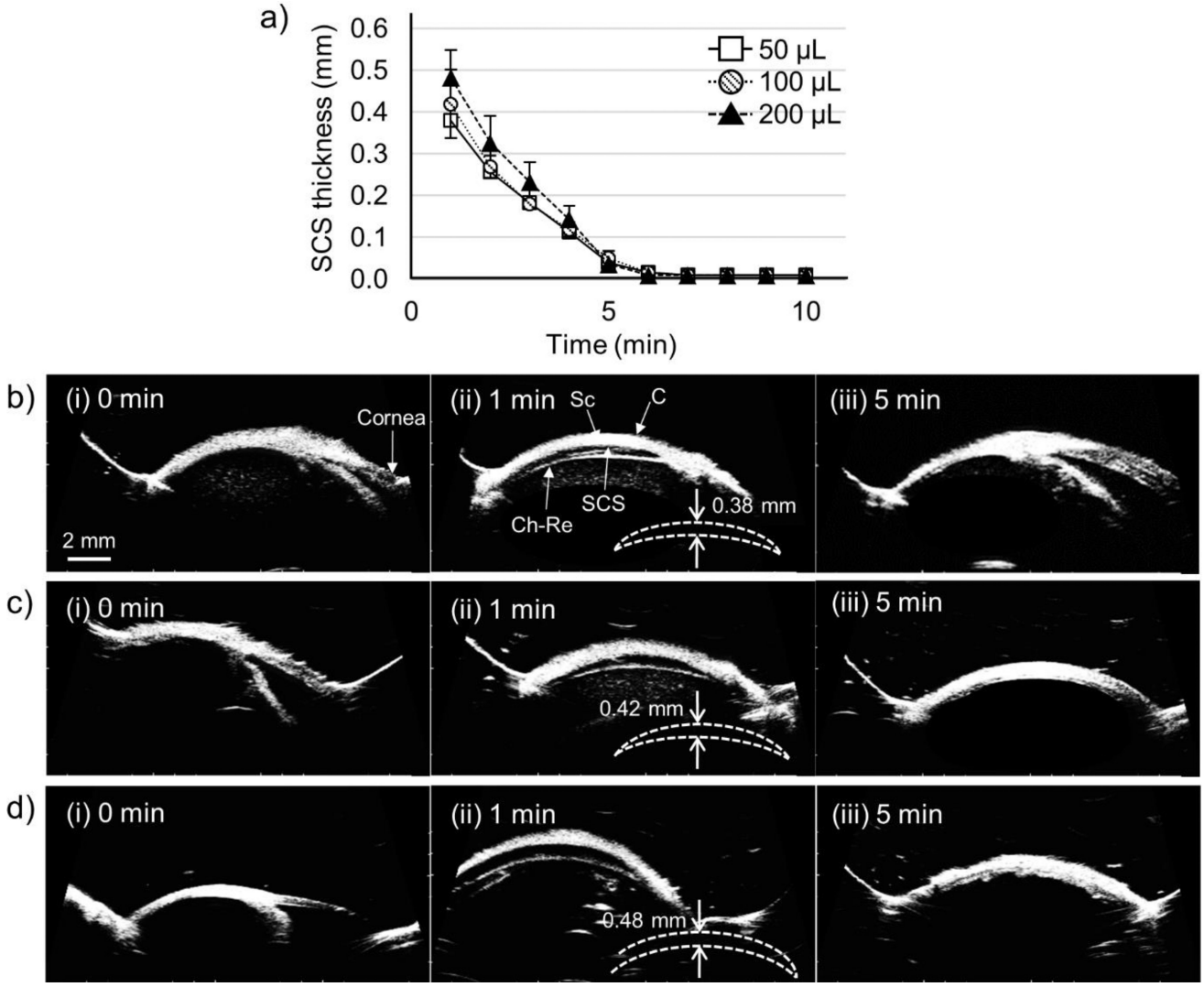

Figure 5.

Expansion and recovery of the suprachoroidal space (SCS) after injection into the SCS of the rabbit eye ex vivo. (a) SCS thickness over time after injection of 50, 100, and 200 µL HBSS containing nanoparticles. Data show average ± standard deviation based on 3 replicate samples. Representative ultrasound images of the rabbit eye (i) 0, (ii) 1, and (iii) 5 min after injection of (b) 50 µL, (c) 100 µL, and (d) 200 µL of HBSS containing nanoparticles. Imaging was performed by B-scan ultrasound, with the probe placed at the site of injection in the supranasal direction of the eye. Sc = sclera, C = conjunctiva, Ch-Re = choroid-retina. Sketches show outline of SCS and expansion distance.

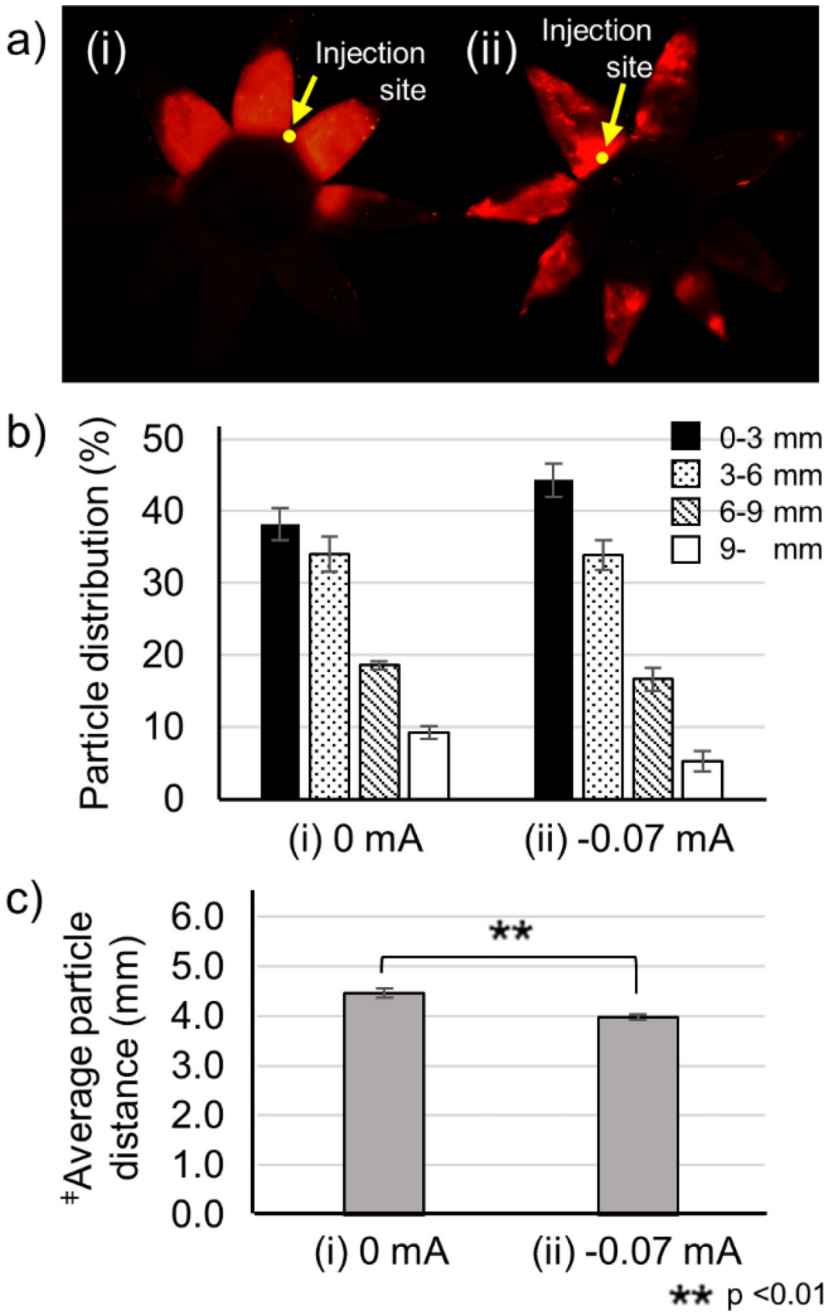

Figure 6.

Effect of iontophoresis polarity after injection of nanoparticles in the suprachoroidal space (SCS). Representative fluorescence micrographs (a), distribution of red-fluorescent nanoparticles in the SCS (b), average distance of nanoparticle transfer in the SCS (c) after injection of 100 μL of nanoparticles in HBSS into the SCS of rabbit eyes ex vivo (i) without iontophoresis (0 mA) and (ii) with iontophoresis at −0.07 mA for 3 min. Fluorescence micrographs (a) show representative flat mounts of the eye after dissection with radial cuts from the posterior pole to the limbus. Yellow arrows point to sites of injection into the SC S.

‡Average particle distance (APD) (mm). Graphs (b and c) present average ± standard deviation based on 3 replicate samples.

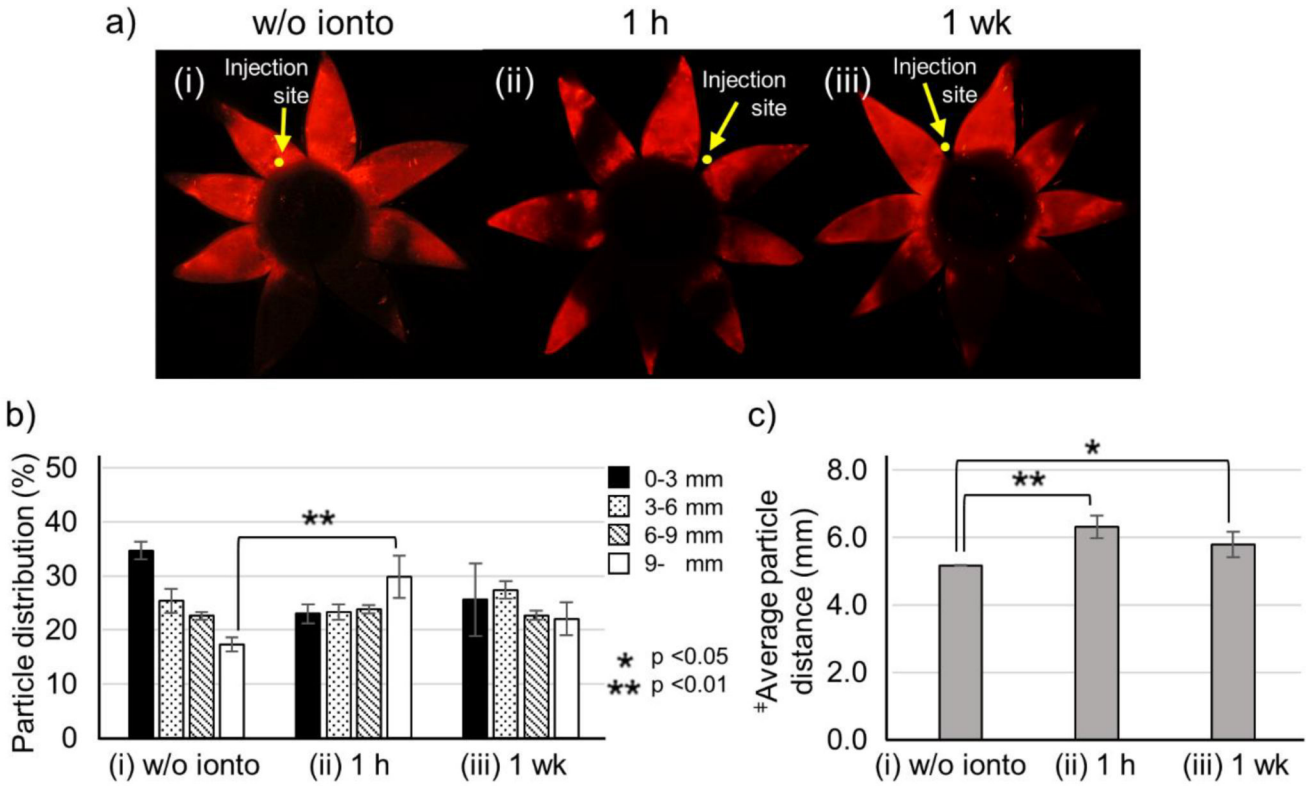

Figure 7.

Effect of iontophoresis after injection of nanoparticles in the suprachoroidal space (SCS) of rabbit eyes in vivo. Fluorescence micrographs (a), distribution of red-fluorescent nanoparticles in the SCS (b), average distance of nanoparticle transfer in the SCS (c) deter mined after injection of 100 μL of nanoparticles in HBSS into the SCS of rabbit eyes in vivo (i) without iontophoresis and (ii) 1 hour and (iii) 1 week after injection with iontophoresis at 0.14 mA for 3 min. Fluorescence micrographs (a) show representative flat mounts of the eye after dissection with radial cuts from the posterior pole to the limbus. Yellow arrows point to sites of injection into the SCS. ‡Average particle distance (APD) (mm). Graphs (b and c) present average ± standard deviation based on 3 replicate samples.